

The use of an improved atmospheric correction algorithm for removing atmospheric effects from remotely sensed images using an atmosphere–surface simulation and meteorological data

D. G. Hadjimitsis^{a*} and C. R. I. Clayton^b

^a Assistant Professor, Cyprus University of Technology, Department of Civil Engineering and Geomatics, Faculty of Engineering and Technology, Lemesos, Cyprus

^b Professor, University of Southampton, School of Civil Engineering and the Environment, Highfield, Southampton, SO17 1BJ, UK

ABSTRACT: Unless effective corrections can be applied, satellite remote sensing data will remain modified by the absorption and scattering effects of the atmosphere through which the electromagnetic radiation must pass, between the Sun, the ground and the sensor. The true reflectance of the land will not be recoverable, and multi-temporal datasets will not be comparable as a result of the variability of the atmosphere. This article presents a method of removing atmospheric effects from satellite remote sensing images for low-reflectance areas, such as water, where the atmosphere accounts for the majority of the at-satellite measured radiance in the visible bands. The method uses visibility observations to select a reference image for the area of interest. The reflectance of the dark target is calculated after atmospheric correction from the reference image, and is used in conjunction with Turner and Spencer's atmosphere–surface simulation (Turner and Spencer, 1972) and Forster's method (Forster, 1984), to correct the remainder of the images. The method is applied to three large water treatment reservoirs to the west of London. Copyright © 2008 Royal Meteorological Society

KEY WORDS atmospheric correction; aerosol optical thickness; meteorological parameters; satellite remote sensing

Received 23 October 2007; Revised 15 April 2008; Accepted 18 April 2008

1. Introduction and background

Satellite remote sensing data are modified by the absorption and scattering effects of the atmosphere. Such interactions occur as the electromagnetic radiation passes between the Sun and the Earth's surface, and the ground and sensor. Unless accurate yet practical methods of atmospheric correction are available, the true reflectance of the land surface cannot be recovered. Indeed, multi-temporal datasets cannot be used, as a result of the variability of the atmosphere, to observe changes in surface properties. This is particularly true for low-reflectance surfaces such as water, where remote sensing monitoring of water quality may be prevented as a result of atmospheric interventions (Hadjimitsis *et al.*, 2004).

Many atmospheric correction methods have been proposed for use with multi-spectral satellite imagery (Hadjimitsis, 1999; Hadjimitsis *et al.*, 2004). They include image-based methods (Ahern *et al.*, 1979; Hadjimitsis *et al.*, 2003), methods that use atmospheric modelling (Vermote, 1996) and finally those that use ground data during the satellite overpass (Moran *et al.*,

1992). Aerosol optical thickness is the key parameter in any atmospheric correction method and other investigators provide several techniques for its determination. There are basically two ways to determine the aerosol optical thickness for removing atmospheric effects from satellite images: (1) using image-based techniques such as the 'dark object' method (for example, Ahern *et al.*, 1979), or 'ocean method' applied over clear water, which considers that 'black oceans' (Morel and Prieur, 1977) are totally absorbing in infrared and near-infrared wavelengths (for example, Griggs, 1975), and the 'dark vegetation method' (for example, Kaufman and Sendra, 1988; Holben *et al.*, 1992); (2) using other auxiliary information such as meteorological parameters (for example, Forster, 1984).

The difficulty of determining the aerosol optical thickness provides the opportunity to researchers to apply either image-based atmospheric correction techniques or corrections that use atmospheric models or radiative transfer (RT) codes (Hadjimitsis *et al.*, 2004). A typical example of image-based correction is the darkest pixel (DP) method, which requires no external data and is the easiest to implement. However, there is some evidence that the use of RT codes and atmospheric modelling (Turner and Spencer, 1972; Turner, 1973; Vermote, 1996) in conjunction with field measurements of aerosol optical

*Correspondence to: D. G. Hadjimitsis, Assistant Professor, Cyprus University of Technology, Department of Civil Engineering and Geomatics, Faculty of Engineering and Technology, Lemesos, Cyprus. E-mail: d.hadjimitsis@cut.ac.cy; dhadjimitsis@cytanet.com.cy

thickness can yield more accurate atmospheric corrections than can be obtained using simple image-based techniques (Moran *et al.*, 1992; Vermote, 1996).

It is, however, impractical to measure the aerosol optical thickness (for example, using ground-based Sun photometers), since this can be a highly variable parameter both temporally and spatially. In the absence of any other data for aerosol size distribution and aerosol optical characteristics, aerosol optical depth can be estimated using the visibility concept, as shown by Forster (1984). Indeed, in the atmosphere–surface simulation and RT calculations algorithm presented by Forster (1984) the aerosol optical thickness was determined on the basis of the available visibility data at the satellite overpass, rather than direct measurement.

Over water bodies, atmospheric effects account for the majority of the at-satellite measured radiance in the visible bands, and therefore such targets provide an opportunity to assess the effectiveness of the different available atmospheric correction methods. This has been shown by Hadjimitsis *et al.* (2004), who provided a critical assessment of the effectiveness of most of the available atmospheric correction algorithms using Landsat TM satellite imagery and *in situ* spectroradiometric measurements. They found that the standard generic models of the atmosphere included in the atmospheric correction methods, such as those suggested by Forster (1984), were not sufficiently accurate when dealing with dark targets such as water bodies.

Most atmospheric correction methods, including Forster's method, did not perform well when comparing corrected satellite-derived reflectances with the range of values to be expected at ground level. The simplest, the DP correction method, provided a reasonable correction in Landsat TM bands 1, 2, and 3, at least for cloud-free scenes (Hadjimitsis *et al.*, 2004).

The DP correction method that has been incorporated in the proposed methodology assumes that the pixel with the lowest digital number (DN) or radiance in each band should in reality be zero and therefore its radiometric DN or radiance value represents the atmospheric additive effect (Hadjimitsis *et al.*, 2003). The DP may correspond to a large water body or other dark object within the scene. The principle of the DP approach is that most of the signal reaching a satellite sensor from a dark object is contributed by the atmosphere at visible wavelengths. Therefore, the pixels from dark targets are indicators of the amount of upwelling path radiance in that band. The atmospheric path radiance adds to the surface radiance of the dark target, giving the target radiance at the sensor. The surface radiance of the dark target is approximated as having zero surface radiance or reflectance. A recent adaptation of the DP method is to assume a known non-zero surface reflectance of the dark target. The main characteristic of dark objects is the very-near-zero radiance in the infrared part of the spectrum. This is due to the fact that water absorbs strongly in the near infrared and any scattering effect is negligible.

2. The atmospheric correction algorithm using meteorological parameters

2.1. Forster's atmospheric correction using Turner and Spencer's (1972) atmosphere–surface simulation

Forster's correction algorithm can be divided into two main stages: (1) obtain the following meteorological data: atmospheric pressure, visibility, relative humidity (RH), and temperature; (2) calculate the optical thickness related with Rayleigh scattering, aerosol scattering, and water vapour absorption based on the meteorological data. *Rayleigh optical thickness* is related to atmospheric pressure. The optical thickness associated with Rayleigh scattering (caused by fluctuations in air density) is given for a standard pressure at sea level of 1013.25 hPa (Fraser, 1975; Chahine, 1983; Elachi, 1987; Vermote, 1996). For pressures at any other elevation an altitude correction is required (Chahine, 1983; Forster, 1984). If there is no significant difference between the observed atmospheric pressure and the standard atmospheric pressure, then atmospheric pressure does not have any significant effect on the Rayleigh optical thickness. *Aerosol optical thickness* can be assessed on the basis of the visibility range or visual range. Forster (1984) uses the visual range concept to describe the haze level of the atmosphere due to aerosols, which are heavily concentrated in the lowest portion of the atmosphere. The aerosol optical thickness is determined using the graph of the aerosol optical thickness *versus* visual range provided by Turner and Spencer (1972). The visual range (also termed meteorological range) is defined to be the maximum distance at which objects can be seen by a human observer (Turner *et al.*, 1971; Turner and Spencer, 1972; Turner, 1973, 1975; Sturm, 1981, 1983; Diederer, 1985). *Water vapour optical thickness*, or the absorption effects of water molecules, can be calculated on the basis of the equivalent mass of water vapour in the atmosphere (Forster, 1984; Jensen, 2000; Richards, 2005). These calculations require temperature and humidity measurements. The atmospheric path radiance is then calculated using the total optical thickness, which is the sum of every optical thickness and the background reflectance (the effect of the adjacent land).

By combining the water vapour absorption, aerosol scattering, and Rayleigh scattering at a given wavelength, the total optical thickness of the atmosphere is calculated using Equation (1)

$$\tau(\lambda) = \tau_r(\lambda) + \tau_a(\lambda) + \tau_{\text{H}_2\text{O}}(\lambda) \quad (1)$$

where

$\tau(\lambda)$ is the total optical thickness

$\tau_r(\lambda)$ is the Rayleigh optical thickness

$\tau_a(\lambda)$ is the aerosol optical thickness

$\tau_{\text{H}_2\text{O}}(\lambda)$ is the water vapour optical thickness.

The atmospheric transmittance between the target and the satellite sensor is given in Equation (2):

$$T(\theta_v) \uparrow = \exp(-\tau(\lambda)/\cos\theta_v) \quad (2)$$

By using the correction algorithm given by Turner and Spencer (1972) the atmospheric path radiance can be calculated and the target reflectance at ground level can be retrieved using Equation (3)

$$\rho_{\text{tg}} = \frac{\pi}{T(\theta_v) \cdot E_G} [L_{\text{ts}} - L_P] \quad (3)$$

where

ρ_{tg} is the target reflectance at the ground

E_G is the global irradiance incident on the target (W m^{-2})

L_P is the atmospheric path radiance ($\text{W m}^{-2} \text{ s r}^{-1}$)

L_{ts} is the target radiance at the sensor ($\text{W m}^{-2} \text{ s r}^{-1}$)

$\frac{1}{\pi}$ accounts for the upper hemisphere of solid angle (Lambertian surface)

$T(\theta_v)$ is the atmospheric transmittance between the target and the satellite sensor

θ_v is the nadir view angle of the satellite sensor (or scan angle).

2.2. Modified atmospheric correction algorithm

Hadjimitsis (1999) found that Forster's method works well in atmospheric conditions with insignificant haze conditions and visibility up to 28 km. The only reliable corrected reflectance values that were consistent in all bands were found for an image acquired in southern United Kingdom on 2 June 1985 (summer), which was characterized by the highest visibility (25–28 km) at the time of satellite overpass (Hadjimitsis, 1999; Hadjimitsis *et al.*, 2004).

On the basis of the results of their previous work (Hadjimitsis *et al.*, 2004), the authors suggest the following modifications of Forster's atmospheric correction method with specific required criteria. The modified method is presented in the following steps:

Step 1. The method should be applied for a series of satellite imagery covering the same area of interest.

Step 2. Choose from an available time series of images of the dark (water) target, the one taken at the time of highest visibility (and more than 28 km) according to data from the nearest meteorological station.

Step 3. Determine the aerosol optical thickness using the graph provided by Forster (1984). Run Forster's atmospheric correction method to obtain a reference image, which is assumed to be free from significant atmospheric effects.

Step 4. From the corrected image (free from atmospheric effects), determine the average target reflectance of the dark target (water body) (ρ_{tg}) at the ground level for all visible and near-infrared bands.

Step 5. For each of the remaining images, run the Forster's procedure using the Turner and Spencer (1972) atmosphere–surface simulation. Substitute the ρ_{tg} in Equation (3), which represents the most representative value of the dark target (water body) under clear atmospheric conditions, i.e. under high

visibility values. The only unknown is the aerosol optical thickness after considering all the assumptions made by Forster (1984).

Step 6. Calculate L_{ts} (target radiance at the sensor, $\text{W m}^{-2} \text{ s r}^{-1}$) as the radiance corresponding to the dark target (water body) on the satellite image using the modified version of the DP approach shown by Teillet and Fedosejevs (1995). In very clear conditions, the satellite sensor should detect only the real reflectance (at ground level) at these dark pixels. However, because of atmospheric scattering, these pixels have a non-zero reflectance value, which is the atmospheric path radiance (Equation (3)). This atmospheric path radiance represents a first-order scattering component (haze), which can be subtracted from the particular band (Hadjimitsis *et al.*, 2003). The assumption behind this proposed method is based on the fact that the image contains at least a few pixels that correspond to dark objects. The DP technique assumes that there is a high probability that there are at least a few pixels in the image with very low reflectance values whose area is assumed to correspond to black surface with (0% or very low reflectance value). The assumption that there are few pixels in the image with near-zero reflectance is based on the fact that in a single band there are very large number of pixels and the probability to find a dark pixel is very high (Hadjimitsis *et al.*, 2003). For example, for a single Landsat TM image there are up to 45 million pixels and by investigating the histogram distribution of all the pixels there is a high probability of finding one pixel, which may correspond to some dark objects such as a water body (Hadjimitsis *et al.*, 2003). The algorithm terminates when the image window does not have any dark pixels, which is not a very common case in satellite remote-sensed imagery (Hadjimitsis *et al.*, 2003). An option is added for the user to work with the minimum radiance value in each band for any target; however, further testing is required.

Step 7. The final stage is to run the atmospheric correction and the new image corresponds to the corrected one.

3. Study area and auxiliary data

3.1. Study area

The study area is located to the west of London, and includes eight large water reservoirs and a major international airport (Heathrow) as shown in Figure 1. The authors used spectroradiometric measurements made on site, but not at the same time as image acquisition, for comparisons between the reflectance values after applying the atmospheric correction and those at the ground level (Hadjimitsis *et al.*, 2004).

Through comparisons of reflectance within a time series of 12 LANDSAT-5 TM images, the overall impact of atmospheric contributions can be shown. The modified atmospheric correction algorithm was applied to the time series of images, and the results were compared with



Figure 1. Partial scene of the Heathrow area and Lower Thames Valley reservoirs (Landsat-5 TM image acquired on 2 June 1985 displayed in true colour). This figure is available in colour online at www.interscience.wiley.com/ma

those derived using Forster's method in its original form (Hadjimitsis *et al.*, 2004).

3.2. Meteorological data

Some researchers use the visibility value as an input parameter into an atmospheric model. This may give some overestimated values of the aerosol optical thickness and therefore care is required. The meteorological range or visual range has been defined by Kneizys *et al.* (1988) and Bukata *et al.* (1995) using Equation (4) when using the Lowtran code. Lowtran is a low-resolution propagation model and computer code for predicting atmospheric transmittance and background radiance (Kneizys *et al.*, 1983, 1988). However, most often only the observer's visibility V is available. So, Lowtran-6 and -7 (Kneizys *et al.*, 1983, 1988) relate to the meteorological range, V_M , with the surface or observer's horizontal visibility at the ground, V , according to the following equation (Gordon, 1970; Bowker and Davis, 1987).

$$V_M = (1.3 \pm 0.3)V \quad (4)$$

where

V_M is the visual range or meteorological range in km
 V is the observer's visibility value km.

All the alternative multiplicative coefficients that have been extracted from Equation (4), such as 1.0 and 1.6, have been used (Hadjimitsis, 1999). Indeed these coefficients have been multiplied by the visibility values (as shown in Table I) acquired during the satellite overpass. On the basis of the fact that visibility data are acquired every 1 h, an interpolated value has been produced to match the satellite overpass. Interpolation has also been applied for the atmospheric pressure values and

Table I. Visibility data for the dates in which satellite images of Lower Thames Valley area were acquired (station: London Heathrow Airport).

Image date	Visibility (km) at London Heathrow Airport station		
	Visibility at 1000 (km)	Visibility at 1100 (km)	Visibility at satellite overpass (km)
12 April 1984	25	27	25.8
5 March 1985	5	12	7.7
17 May 1985	12	15	13.2
2 June 1985	25	28	26.2
4 July 1985	6	10	7.5
29 September 1985	5	9	6.9
8 October 1985	40	40	40
24 October 1985	7	10	8.1
9 November 1985	20	25	21.8
13 February 1986	9	9	9
8 March 1986	4.5	8	5.9
28 June 1986	5	6	5.4

Table II. Atmospheric pressure data (station: London Heathrow Airport).

Image date	Atmospheric pressure (hPa)		
	Atmospheric pressure at 1000	Atmospheric pressure at 1100	Atmospheric pressure at satellite overpass
12 April 1984	1023.2	1023.2	1023.2
5 March 1985	1023.2	1024.1	1023.6
17 May 1985	1023.4	1023.2	1023.3
2 June 1985	1025.1	1024.6	1024.9
4 July 1985	1016.1	1015.7	1015.9
29 September 1985	1026.5	1026.1	1026.9
8 October 1985	1017.4	1017.6	1017.5
24 October 1985	1028.8	1028.3	1028.6
9 November 1985	1090.5	1090.6	1090.5
13 February 1986	1022.1	1022.0	1022.1
8 March 1986	1025.4	1025.2	1025.3
28 June 1986	1023.1	1021.7	1025.5

relative humidity (RH%) as shown in Tables II and III, respectively.

4. Results

A comparison between the modified methods with Forster's method was performed. Figure 2 shows reflectance values for Queen Mary Reservoir calculated from the at-satellite measurements of radiance, for each of the 12 images. These are compared with values corrected using Forster's method (based on Turner and Spencer's atmosphere-surface model), and with those corrected using the modified method described in this article. Also shown are minimum and maximum values of

IMPROVED ATMOSPHERIC CORRECTION USING METEOROLOGICAL DATA

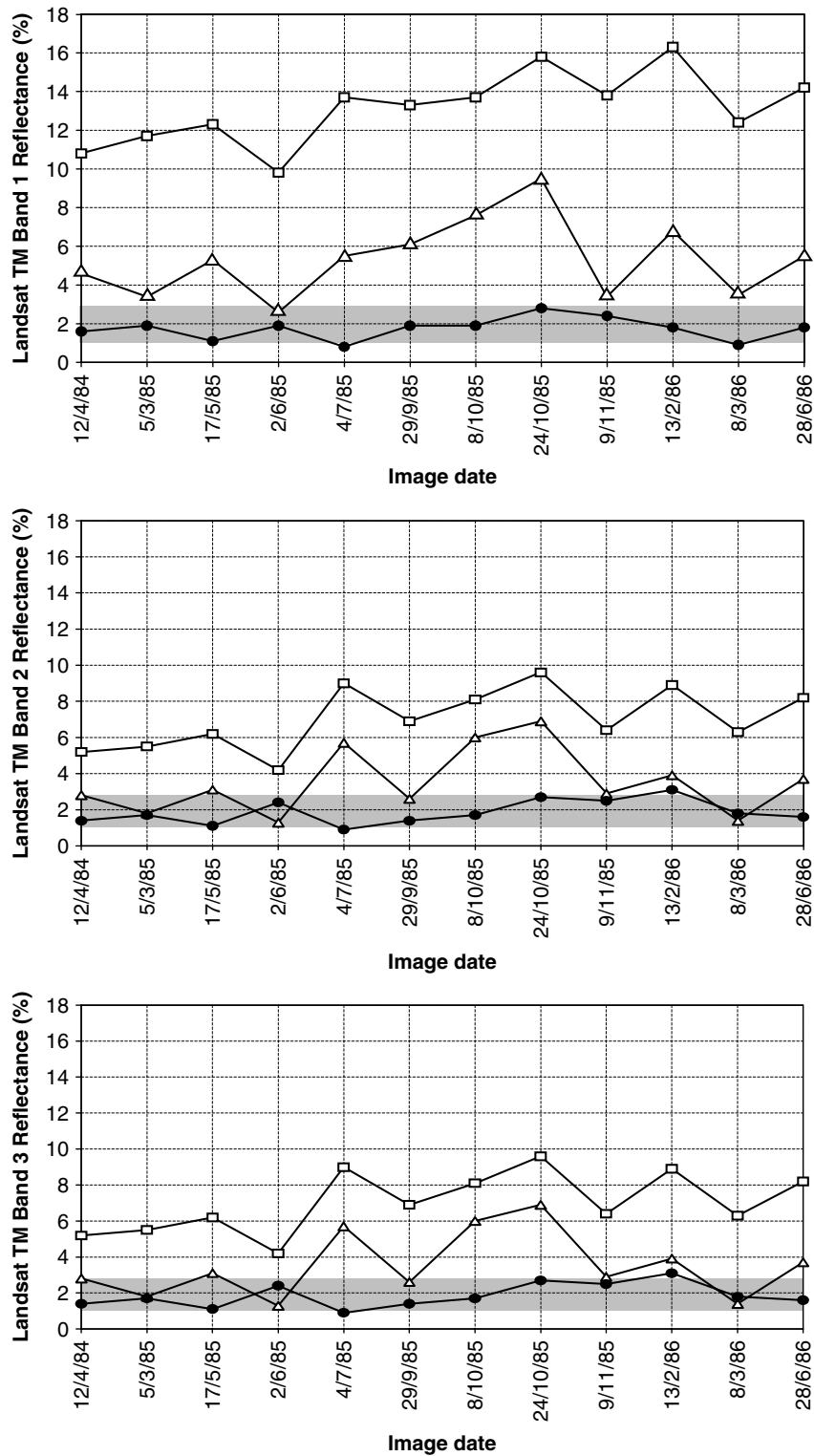


Figure 2. Comparison between measured at-satellite reflectance values, corrected reflectance values and ground data for Queen Mary Reservoir, for Landsat TM band 1 (upper graph), band 2 (middle graph), and band 3 (lower graph). The measured at-satellite reflectance values are shown by the upper line, and open squares. Values calculated using Forster's method are shown by the middle line and open triangles. The shaded area shows the range of *in situ* reflectance values measured using the GER-1500 field spectroradiometer. Values calculated using the proposed new method are shown by the lower line and solid circles.

reflectance calculated from ground measurements made using a GER1500 field spectroradiometer (Hadjimitsis *et al.*, 2004).

It can be seen that Forster's method (Forster, 1984) yields higher values of reflectance when compared with

both the measured maximum and the values calculated from the satellite data using the modified method. This suggests that it does not remove the atmospheric effects completely. It appears that for visibility less than 28 km, Forster's method does not provide sufficient correction.

Table III. Relative humidity (%) data (calculated on the basis of the acquired dry- and dew-point temperatures).

Image date	Relative Humidity (RH)%		
	RH (%) at 1000	RH (%) at 1100	RH (%) at satellite overpass
12 April 1984	57	50	54.2
5 March 1985	82	76	79.7
17 May 1985	55.5	52	54.1
2 June 1985	59	49	55.0
4 July 1985	64.5	53.5	60.4
29 September 1985	72	64	68.4
8 October 1985	66	51	60.8
24 October 1985	71	54	65.1
9 November 1985	82	87	83.8
13 February 1986	51	51	51.0
8 March 1986	75	61.5	69.4
28 June 1986	54	48	51.6

Although it does improve the correspondence between calculated and estimated ground reflectance, the results are scattered and variable across the time series of images, especially in Landsat TM bands 1, 2, and 3. Landsat TM band 4 was not used since the DP approach was found to work more efficiently in the other three bands (Hadjimitsis *et al.*, 2003).

The modified method gives results that are generally in agreement with those calculated from field measurements (within the minimum and maximum values of field measurements). The overall average corrected reflectance values from the 12 images was 1.7, 2.4, and 1.9% as compared with an average value from field measurements of 1.8, 3.2, and 1.9% for TM bands 1, 2, and 3.

5. Conclusions

A modified atmospheric correction method is presented to optimize atmospheric correction for satellite remote sensing for areas consisting of dark low-reflectance objects, such as inland waters.

It is proposed that the image taken under highest visibility conditions, and with a visibility in excess of 28 km as identified from local meteorological data, is utilized to quantify the aerosol optical thickness, to produce a 'reference image' that (following atmospheric correction using Forster's (1984) method) is assumed to have reflectance values free from atmospheric effects. The reflectance value at ground level is extracted from this image for the selected dark target. This is used as an input parameter for running the atmosphere-surface simulation and Forster's method on the other images.

By comparing the corrected at-satellite and estimated ground reflectance values in three large water treatment reservoirs, improved corrected values of reflectance were found in the TM bands 1, 2, and 3, when compared with the values produced using Forster's method. The modified method gave values of reflectance similar to those calculated on the basis of field spectroradiometer data.

Further research is required to provide more validation results and estimates of the possible errors that may be encountered. The use of more meteorological stations in the area under investigation may improve the accuracy of the method, since possible large spatial variations of atmospheric effects may have occurred.

Acknowledgements

We gratefully acknowledge Thames Water Utilities (Walton-on-Thames) for their financial support and for their technical support during the spectroradiometric measurements in the Lower Thames Valley reservoirs. The authors acknowledge the support of the NERC Equipment Pool for Field Spectroscopy (EPFS) for providing the GER1500 field spectroradiometer, as well the Meteorological Offices at Bracknell and Heathrow stations.

References

- Ahern FJ, Goodenough DG, Jain SC, Rao VR. 1979. Use of clear lakes as standard reflectors for atmospheric measurements. In *Proceedings of the 11th International Symposium on Remote Sensing of Environment*. Ann Arbor, 731–755.
- Bowker DE, Davis RE. 1987. Effects of aerosols and surface shadowing on bi-directional reflectance measurements of deserts. NASA Technical Paper: 2765, p 4.
- Bukata RP, Jerome JH, Kondratyev KY, Pozdnyakov DV. 1995. *Optical Properties and Remote Sensing of Inland and Coastal Waters*. CRC Press: Boca Raton, FL, USA.
- Chahine MT. 1983. Interaction mechanisms within the atmosphere (Chapter 5). In *Manual of Remote Sensing*, 2nd edn, Colwell RN (ed.). American Society of Photogrammetry: Falls Church, VA; 165–230.
- Diederer A. 1985. Visibility reduction by air pollution in the Netherlands. *Aerosol Science and Technology* **19**(2): 377–383.
- Elachi C. 1987. *Introduction to the Physics and Techniques of Remote Sensing*. John Wiley and Sons: New York.
- Forster BC. 1984. Derivation of atmospheric correction procedures for Landsat MSS with particular reference to urban data. *International Journal of Remote Sensing* **5**(5): 799–817.
- Fraser RS. 1975. Interaction mechanisms within the atmosphere (Chapter 5). In *Manual of Remote Sensing*, 1st edn, Reeves RG (ed.). American Society of Photogrammetry: Falls Church, VA; 165–230.
- Gordon JI. 1970. Daytime Visibility. A conceptual Review. AFGL-TR-0257, AD A0854551.
- Griggs M. 1975. Measurements of atmospheric optical thickness over water using ERTS-1 Data. *Journal of Air Pollution Control Association* **25**: 622–626.
- Hadjimitsis DG. 1999. The application of atmospheric correction algorithms in the satellite remote sensing of reservoirs. PhD thesis. University of Surrey, School of Engineering in the Environment, Department of Civil Engineering, Guildford.
- Hadjimitsis DG, Clayton CRI, Hope VS. 2004. An assessment of the effectiveness of atmospheric correction algorithms through the remote sensing of some reservoirs. *International Journal of Remote Sensing* **25**(18): 3651–3674.
- Hadjimitsis DG, Clayton CRI, Retalis A. 2003. Darkest pixel atmospheric correction algorithm: a revised procedure for environmental applications of satellite remotely sensed imagery. In *Proceedings 10th International Symposium on Remote Sensing*, 8–12/9/2003, Barcelona, organised by NASA, SPIE CONFERENCE, 414.
- Holben BE, Vermote E, Kaufman YJ, Tanre D, Kalb V. 1992. Aerosol retrieval over land from AVHRR Data. *IEEE Transactions on Geoscience and Remote Sensing* **30**: 212–222.
- Jensen JR. 2000. *Introductory Digital Image Processing*. Prentice Hall: NJ, USA.
- Kaufman YJ, Sendra C. 1988. Algorithm for automatic atmospheric corrections to visible and near-IR satellite imagery. *International Journal of Remote Sensing* **9**(8): 1357–1381.

- Kneizys FX, Shettle EP, Gallery WO, Chetwynd JH, Abreu LW, Selby JEA, Clough SA, Fenn RW. 1983. *Atmospheric Transmittance/Radiance: Computer Code LOWTRAN 6*. Air Force Geophysics Laboratory: Hanscom Air Force Base, MA.
- Kneizys FX, Shettle EP, Abreu LW, Chetwynd JH, Anderson GP, Gallery WO, Selby J, Clough SA. 1988. User's guide to LOWTRAN 7. Air Force Geophysics Laboratory, Hanscom AFB Environmental Research Report ERP No.1010.
- Moran MS, Jackson RD, Slater PN, Teillet PM. 1992. Evaluation of simplified procedures for retrieval of land surface reflectance factors from satellite sensor output. *Remote Sensing of Environment* **41**: 169–184.
- Morel A, Prieur L. 1977. Analysis of variations in ocean color. *Limnology and Oceanography* **22**: 709–722.
- Richards JA. 2005. *Remote Sensing Digital Image Analysis: An Introduction*, 4th edn. Springer-Verlag: Berlin.
- Sturm B. 1981. The atmospheric correction of remotely sensed data and the quantitative determination of suspended matter in marine water surface layers. *Remote Sensing in Meteorology, Oceanography and Hydrology* **147**: 163–197.
- Sturm B. 1983. Selected topics of coastal zone colour scanner (CZCS) data evaluation. In *Remote Sensing Applications in Marine Science and Technology*, Cracknell AP (ed.). REIDEL: Scotland, 137–167.
- Teillet PM, Fedosejevs G. 1995. On the dark target approach to atmospheric correction of remotely sensed data. *Canadian Journal of Remote Sensing* **21**(4): 375–381.
- Turner RE. 1973. Atmospheric effects in remote sensing. In *Remote Sensing of earth Resources*, Shahrkhi F (ed.). Technical papers selected from the Conference of Earth Resources Observation and Information Analysis System: Tullahoma, TN; 549–583.
- Turner RE. 1975. Signature variations due to atmospheric effects. In *Proceedings of the 10th International Symposium on Remote Sensing of the Environment, II Michigan*, Ann Arbor, 671–682.
- Turner RE, Malila WD, Nalepka RF. 1971. Importance of atmospheric scattering in remote sensing or everything you've wanted to know about atmospheric scattering but we are afraid to ask. In *Proceedings of the seventh International Symposium on Remote Sensing of the Environment, III Michigan*, Ann Arbor, 1651–1695.
- Turner RE, Spencer MM. 1972. Atmospheric model for correction of spacecraft data. In *Proceedings of the eighth International Symposium on Remote Sensing of the Environment, II. Michigan*, Ann Arbor; 895–934.
- Vermote E. 1996. Atmospheric Correction Algorithm: Spectral Reflectances (MOD09). Algorithm Technical Background Document. NASA5-96062.